

PAPER • OPEN ACCESS

Hydrodynamic design of rotor blades of marine current turbines

To cite this article: F Perez Arribas 2019 *IOP Conf. Ser.: Earth Environ. Sci.* **354** 012004

View the [article online](#) for updates and enhancements.

Hydrodynamic design of rotor blades of marine current turbines

F Perez Arribas^{1,2}

¹Naval Architecture School of Madrid, Universidad Politécnica de Madrid (UPM), Spain

E-mail: francisco.perez.arribas@gmail.com

Abstract. The utilisation of marine current turbines with horizontal axis for electrical power production offers a sustainable and clean option to augment traditional energy technologies and enhance the expansion of renewable energies in the marine field. Some prototypes of these turbines are now available and operating. The advantages of tidal currents for renewable energies when compared with wind resources are that sea water is about 800 times denser than air (and the extracted energy is proportional to density) and the nature of currents that results in a more predictable resource than wind resources. But these advantages set certain limitations and technical problems, some of them related with the hydrodynamic design of rotor blades since the design of a marine turbine is some kind different of the techniques used for wind turbines. Methodologies need be established to describe the physical and operational performance of the turbines, allowing their design to be investigated and performance evaluated. This paper describes the hydrodynamics of rotor design that is projected in order to extract the maximum power from the tide. The blade element momentum theory is used for the rotor modelling, different aspects and limitations of this approach when applied to marine rotor design are commented, and examples are presented.

1. Introduction

Oceans are a substantially resort of renewal energies, well in form of thermal or in kinetic energy (waves and currents). There are different ways to obtain kinetic energy from tidal currents, which can be converted into electricity using marine current turbines (MCT) technology, in a similar way that inland wind turbines extract energy from air currents.

Like in wind energy, ocean energy resource is only economically practicable in some specific sites of the world, where the currents are strong enough to produce a profitable amount of energy, since energy varies with the third power of the current speed. However, this production can make a respectable amount of energy supply and is the reason why marine renewable sector are the focus of industrial and academic research.

In May 2003, the prototype “SeaFlow” (figure 1) from Marine Current Turbines Ltd. was installed off the coast of Lynmouth, North Devon, England. Seaflow was a single rotor turbine which generated 300 kW. The successor of Seaflow was SeaGen, a 1.2 MW double rotor turbine.

Verdant Power developed the RITE project in New York City’s East River. This is a 35 kW turbine in prototype stage (figure 2) for a future commercial development.



Content from this work may be used under the terms of the [Creative Commons Attribution 3.0 licence](#). Any further distribution of this work must maintain attribution to the author(s) and the title of the work, journal citation and DOI.



Figure 1. “SeaFlow” from MCT ltd.



Figure 2. The RITE project from Verdant Power.

This paper describes the hydrodynamics of rotor design that is projected in order to extract the maximum power from the tide and convert it into (usually) electricity. The rotor is the first element in the chain of functional elements of a turbine and it has a decisive influence on the entire system.

Although wind turbine technology has set the foundation to describe the physical and operational performance of the marine turbines, there are a number of fundamental differences in the design and operation of a marine turbine that require research.

The performance of a marine current turbine can be modelled satisfactorily using blade element momentum (BEM) theory. This results from the use of high aspect ratio blades for which the resulting flow is close to 2D over the blade sections before stall, neglecting 3D flow between the turbine annular sections.

2. How much energy is in a fluid

Since the primary purpose of a turbine (Horizontal Axis Turbine) is to convert the kinetic energy (KE) of a fluid into electricity, the first step is to consider how much energy is available. Suppose the fluid advancing from left to right at a constant speed U_0 , for simplicity, let's assume that the fluid is steady (not varying in time) and uniform (not varying in position) and perpendicular to the blade disk. These assumptions are normally used in rotor design, although turbulence and non-uniformity have to be considered in a further stage of the hydrodynamic studies. These circumstances are not considered in this paper.

The fluid will have a constant density that means that the flow is incompressible. The blade radius will be denoted as R , and the turbine can be represented by a circular disk whose area $A = \pi R^2$ represents the blades (figure 3)

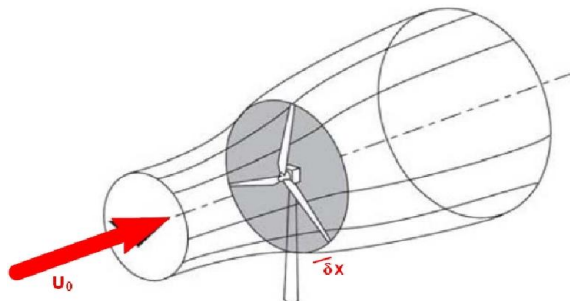


Figure 3. Energy flow through a circular disk.

On figure 3, the disk represents an elemental volume of the flow. The volume of this element is the product of $A \cdot \delta x$, so its mass will be $\rho \cdot A \cdot \delta x$ and its KE will be $0.5 \cdot \rho \cdot A \cdot \delta x \cdot U_0^2$. The time taken for this element to cross the blade disk is given by $\delta x = U_0 \cdot \delta t$ and the contribution of the element to the total amount of KE that passes in δt is given by:

$$\delta(KE) = \frac{1}{2} \cdot \rho \cdot A \cdot U_0 \cdot \delta t \cdot U_0^2 = \frac{1}{2} \cdot \rho \cdot A \cdot U_0^3 \cdot \delta t \quad (1)$$

So the amount of kinetic energy that passes the blade disk per unit of time will be the available power from the fluid:

$$\frac{\delta(KE)}{\delta t} = \dot{W} = \frac{1}{2} \cdot \rho \cdot A \cdot U_0^3 \quad (2)$$

Equation (2) indicates that the power of a turbine depends on the cube of the fluid velocity and on its density [1]. In practice the power output is never as great as suggested in (2) that will be only reached when the fluid is decelerated to rest. Furthermore, a turbine cannot capture all the flow crossing the disk since the flow expands before the disk, reducing its speed, and the flow lines are deflected. Betz proved in 1920 that there is a limit of efficiency of 0.593, and in real practice turbines are below an efficiency of 0.5 without considering electrical and mechanical losses. This efficiency is often referred as the power coefficient C_p :

$$C_p = \frac{W}{\frac{1}{2} \cdot \rho \cdot A \cdot U_0^3} \quad (3)$$

In reality, a rotor will impart a rotating motion or spin to the rotor wake, and the energy contained in this spin reduces the useful proportion of the total energy. This is explained later when the mathematical modelling of the rotor will be explained.

3. Tidal currents

When considering tidal currents, two facts are noticeable: seawater is 800 denser than air and tidal currents are utterly predictable (sailors have charted them for centuries). Tidal currents are mainly independent of weather conditions and are accurate foreseeable, while solar and wind energies can not be predicted with confidence.

The tides cause water to flow inwards (flood flow) and seawards (ebb flow) twice a day. This will produce a periodical flow in the turbine area. The flow pattern caused by tidal influence is much more difficult to analyse, and also, data is much more difficult to collect. A tidal height is a simple number which applies to a wide region simultaneously. A flow has both a magnitude and a direction, which both can vary substantially over just a short distance due to local bathymetry, and also vary with depth below the water surface. Flood and ebb flows are often not in opposite directions. The direction of a flow is determined by the shape of the channel it is coming from, not the shape where it will shortly be. Likewise, eddies can form in one direction but not the other. So, the speed diagram for a given position has normally an elliptical shape.

Because of these reasons, there are some places in the world, that are most suitable than others for the installations of MCT because of its current speed, such as Raz de Sein or Raz Blanchard in France, the Strait of Messina in Italy, the bay of Fundy in Canada.

Power generation is possible for most of the tidal cycle. This may be true in principle since the time of still water is short, but in practice turbines lose efficiency at partial operating powers. Since the power available from a flow is proportional to the cube of the flow speed, the times during which high power generation is possible turn out to be rather brief unless a yaw mechanism orients the rotor towards the current or several tidal power generation stations are used, at locations where the tide phase is different enough so that low power from one station is filled in by high power from another.

4. Modeling the rotor

When studying a rotor, forces acting on the blades, which give rise to the thrust and torque and

hence power, have to be computed. The blade element momentum theory (BEM) established by Glauert will be used to study the rotor blades.

The rotor is substituted by an actuator disk (figure 3) that supports a pressure difference and decelerates the current through the disk. This is also equivalent to consider a rotor of an infinite number of blades.

The velocity will be decreased at the rotor to $U_1 = U_0 \cdot (1-a)$, and downstream the current is slowed further to $U_\infty = U_0 \cdot (1-2 \cdot a)$. The velocity at the rotor is considered the average between the current and the downstream velocities. The axial induction factor a reflects the decreasing in current velocity at the rotor:

$$a = \frac{U_0 - U_1}{U_0} \quad (4)$$

The power extracted by the rotor will be:

$$\begin{aligned} W &= \frac{1}{2} \cdot \rho \cdot A \cdot U_0 \cdot (U_1 - U_\infty) \cdot (U_1 + U_\infty) = \\ &= \frac{1}{2} \cdot \rho \cdot A \cdot U_0^3 \cdot 4 \cdot a \cdot (1-a)^2 \end{aligned} \quad (5)$$

And the power coefficient of equation (3) can be calculated as a function of a :

$$C_p = \frac{W}{\frac{1}{2} \cdot \rho \cdot A \cdot U_0^3} = 4 \cdot a \cdot (1-a)^2 \quad (6)$$

A little work on equation (6) will produce the mentioned Betz limit of 0.593 for $a = 1/3$. Additional calculations can be derived to obtain the thrust of the tide on the rotor:

$$T = \frac{1}{2} \cdot \rho \cdot A \cdot (U_0^2 - U_\infty^2) = \frac{1}{2} \cdot \rho \cdot A \cdot U_0^2 \cdot 4 \cdot a \cdot (1-a) \quad (7)$$

And a thrust coefficient is obtained:

$$C_T = \frac{T}{\frac{1}{2} \cdot \rho \cdot A \cdot U_0^2} = 4 \cdot a \cdot (1-a) \quad (8)$$

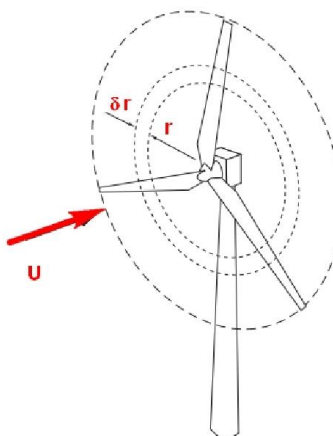


Figure 4. Annular streamtube.

The traditional way to extend the previous expressions from the actuator disk to the turbine blades is to divide the flow through the blades into a number of concentric annular streamtubes or strips along the span, and consider these elements as control volumes, figure 4. The intersection between the streamtubes and the turbine will be the blade elements and velocity and forces within each stream tube can be calculated with the premise that the flow in each streamtube is independent of that in another streamtube.

Another assumption of BEM is that the blade elements behave as airfoils. If a blade element at radius r is considered, the 2D analogy will be an infinite cascade of airfoils spaced $2\pi r/N$, where N is the number of blades. The ratio of the element's chord length c to this quantity is called solidity $\sigma = N \cdot c / (2\pi r)$. For low solidity, the blade would behave as an airfoil, but for high values of solidity the flow over each blade will be affected by the proximity of the adjacent blades. Nevertheless, this solidity is low enough for the calculations because of the slender shape of turbine blades.

With the momentum theory, one can calculate the induced velocities from the momentum lost in the axial and tangential directions for a given annular streamtube. The contribution to the thrust of a blade element can be calculated as:

$$dT = \rho U_0^2 \cdot 2\pi r_0 \cdot \delta r_0 - \rho U_\infty^2 \cdot 2\pi r_\infty \cdot \delta r_\infty = \\ = 4\pi \rho U_0^2 \cdot a \cdot (1-a) \cdot \delta r \quad (9)$$

The torque of a blade element is calculated with the help of conservation of the angular momentum:

$$dQ = \rho r_\infty W_\infty U_\infty \cdot 2\pi r_\infty \cdot \delta r_\infty$$

Where W_i stands for a swirl velocity, related with the circulation around the airfoil. The previous expression assumes that there is no swirl upstream of the blades. If the angular momentum is conserved downstream, it means $r \cdot W_i = r_\infty \cdot W_\infty$ so, the torque contribution can be rewritten as:

$$dQ = 2\pi \rho U_0 \cdot (1-a) \cdot W_i \cdot r^2 \cdot \delta r = \\ = 4\pi \rho U_0 \cdot (1-a) \cdot a' \Omega \cdot r^3 \cdot \delta r \quad (10)$$

Where $W_i = 2a' \Omega r$, defining a' as the rotational interference factor and Ω as the turning ratio (rad/s). If a indicates the decreasing of current velocity in the rotor blades, a' represents the effect on the fluid of the turning of the blades that will be accelerated contrary to the rotating direction.

4.1. Forces acting on a blade element

One of the assumptions of the BEM is that the blade elements behave as airfoils, which combined with the analysis of the previous section allows the calculation of the forces acting on a blade element.

For a blade element at a radius r , the velocities and forces acting on it are depicted in figure 5. The undisturbed current velocity is U_0 but it has to be corrected because of the speed losses at the rotor with a term $U' = a \cdot U_0$, so the velocity of the water is $U_1 = (1-a) \cdot U_0$.

The circumferential or tangent velocity is $T = \Omega \cdot r$, but the effect of turning in the fluid produces the term $T' = a' \cdot \Omega \cdot r$. The combination of both axial and tangent components produces the velocity polygon of figure 5. With this polygon, the total or effective velocity W as seen by the blade element can be computed.

This figure shows also some important angles. The first one is β and it is the geometrical angle between the plane of rotation and the element's chord line. It is imposed by the designer and is called twist angle. The second angle is α , the angle of attack of the water to the profile. And finally, the third angle shows the incidence angle of the total speed W in respect to the rotor plane, and is

the sum of the previous angles: $\varphi = \alpha + \beta$

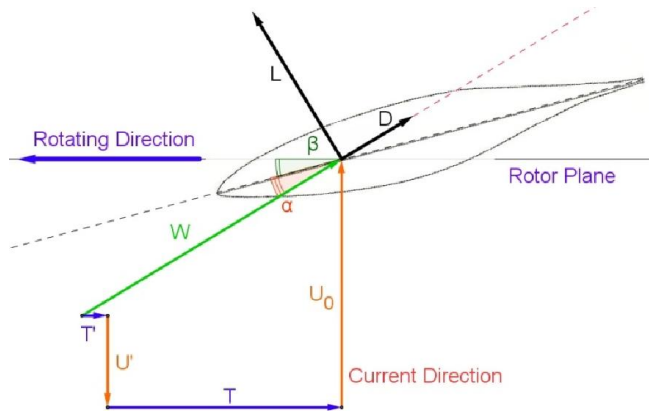


Figure 5. Velocities and forces for a blade element.

The effect of the total velocity with α angle of attack will produce a force that is decomposed in two: Lift (L) and Drag (D), perpendicular and parallel to the flow direction.

The magnitude of $T = \Omega \cdot r$ varies importantly across the blade span, so β has to vary significantly with radius to maintain α at reasonable values to avoid flow separation. Angle β can be altered including pitch controllable blades, so the power can be reduced to avoid over power in case of high flow speed or to adapt the blade to an optimum position that depends of the flow characteristics.

Assuming lift and drag acting on the element are the same as those on an airfoil of the same section, angle of attack and total velocity W , they can be calculated with the use of lift and drag coefficients C_l and C_d and are proportional to the chord c of the profile:

$$L = \frac{1}{2} \cdot \rho \cdot W^2 \cdot C_l \cdot c \quad D = \frac{1}{2} \cdot \rho \cdot W^2 \cdot C_d \cdot c \quad (11)$$

These coefficients can be obtained from experiments in wind or cavitation tunnels, and are tabulated as a function of Reynolds number and angle of attack in the called “polar curves”. There are many references and families of airfoils that include these tables [2].

From the practical point of view, equations (12) and (13) shows that the key of the hydrodynamic design is the selection of appropriate profiles in order to maximize L and minimize D, and also the proper selection of the twist angle, so that every profile along the blade’s length operates at an optimum angle of attack.

With the use of Lift and Drag from equation (11), the total thrust and torque on N blade elements of a turbine can be calculated:

$$dT = \frac{1}{2} \cdot \rho \cdot W^2 \cdot c \cdot N \cdot (C_l \cdot \cos \varphi + C_d \cdot \sin \varphi) \cdot \delta r \quad (12)$$

And

$$dQ = \frac{1}{2} \cdot \rho \cdot W^2 \cdot c \cdot N \cdot (C_l \cdot \sin \varphi - C_d \cdot \cos \varphi) \cdot r \cdot \delta r \quad (13)$$

Equations (12) and (13) are the basic blade element equations. Through and iterative procedure with equations (12) and (9) for the thrust and with equations (13) and (10) for the torque, the axial and the rotational interference factors can be computed, and with these factors, the total velocity W and its correspondent angle of attack allows the interpolation of C_l and C_d to calculate thrust and

torque for a given element at a radius r [3].

Considering several blade elements for different radius r and by integrating their resulting dT and dQ distribution along the blade's span, total hydrodynamic thrust and torque acting on the turbine blades can be worked out.

4.2. Corrections to the theory

Some correction of the mentioned theory comes from realising that the streamtube analysis has assumed that the velocities and pressures are uniform in the circumferential direction, or in other words, the axial velocity at a blade element may be different from U_1 given by equation (4), which is the streamtube's average velocity, Figure 6.

The calculation of the balance of forces includes not only the forces of the blade element, but also other components from the spatial flow around the blade. This is more pronounced next to the blade tip, where the pressure difference between the top and the underside of the blade produces the tip vortices. The result drag is called induced drag. There are equivalent losses next to the turbine hub.

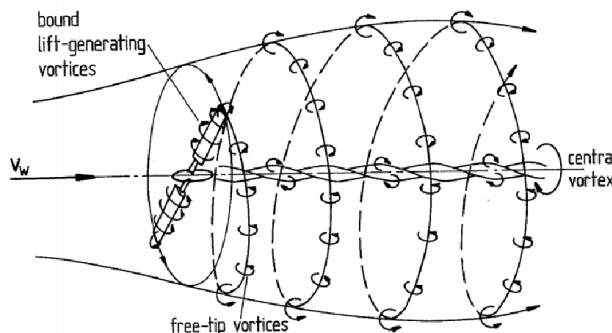


Figure 6. Vortices produced by the rotor.

Semi-empirical corrections factors for the coefficients a and a' such as the ones proposed by Prandtl or Goldstein can be implemented in the theory to model these induced losses [4].

But the most important corrections are considered for high loaded rotors. When a is high, the momentum theory predicts a reversal of the flow in the wake as can be seen in equation (7). Such a situation cannot actually occur so what happens is that the wake becomes turbulent and, in doing so, entrains water from outside the wake by a mixing process which re-energizes the slow moving water which has passed through the rotor. This has been experimentally demonstrated in air (figure 7).

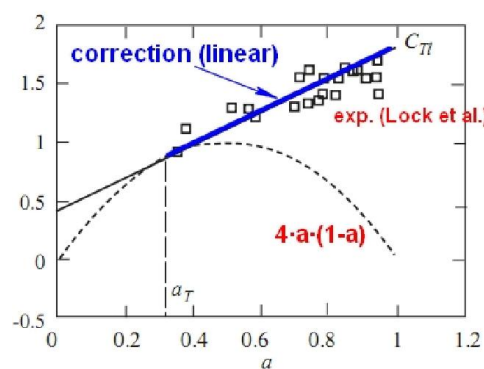


Figure 7. C_T for highly loaded blades.

In a high loaded rotor, $a > 0.4$, the flow will pass from one face of the blade to the other producing swirls, which can not be modelled with the BEM theory. This can be corrected by assuming a new expression for the thrust instead of equation (7) for $a > 0.4$, such as the linear fitting of the experimental data proposed in figure 7.

5. Designing the rotor

When designing a rotor, the task is to find the best possible rotor on the basis of a determined requirements and objectives. The starting point is a certain idea of the power output of the turbine on a given location. This location will be described by an average tidal speed and is a function of the depth where the turbine is installed.

It is out of the scope of this paper to explain the effect of a variable speed profile in the rotor characteristics, or the behaviour of the turbine in a skew condition when the flow is not perpendicular to the rotor plane. Normally a design speed at the depth of the rotor hub, U_0 , is a design parameter. An advantage of the tidal current is that this speed is quite predictable and without big variations as in wind turbines.

With the estimated power and speed, the rotor diameter can be estimated with a rough estimation of the rotor power coefficient. An average value of 0.4 is a common starting point.

Although it is mathematically possible to derive optimum shapes for the rotor blades, this is a merely orientation in the design process, since the final solution will be a compromise between hydrodynamics, strength and economical production, and it is also influenced by other factors such as the installed generator and rotor power control. The final result is achieved after an iterative process, where the hydrodynamics can be studied with the use of BEM theory described in the previous sections.

Since this paper is focused in hydrodynamics, the important factor will be the optimization of the power coefficient and the main parameters dominating C_p will be:

- The number of blades
- Chord and twist distribution of the blades
- Airfoil characteristics

The previous sections have explained how the rotor impart a rotating motion or spin to the rotor wake and how to model this motion mathematically in order to obtain forces and moments. The power, thrust and torque coefficients will be a function of the ratio between the rotating motion and the translation motion of the water flow. This ratio shows the relation between the tangential velocity of the rotor blades and the axial flow and is normally called tip speed ratio:

$$\lambda = \frac{\Omega \cdot R}{U_0} \quad (14)$$

Where Ω are the rpm that are a function of the generator turning speed and of the multiplier that connects them.

5.1. Number of blades

This is the first design parameter to impose, and its influence on rotor power is small. Nevertheless it determines the optimum tip speed ratio where the maximum power is achieved, that is normally the design point of the rotor: a rotor with a lower number of blades rotates faster compensating the smaller blade area.

Figure 8 shows the influence of the number of rotor blades, for blades of identical shape. The maximum value does not change importantly with the number of blades, so rotors with more than 3 blades, are not used.

The optimum λ lies between 7 and 8 for a three blades rotor, and between 9 and 10 for a two blades rotor. So according to the optimum λ of the design, the number of blades is selected.

Notice that according equation (14), for lower tidal flow speeds maintaining constant rpm, the tip speed will be increased, so a 2 blades rotor is less sensitive to the reduction of the power

coefficient than a 3 blades rotor.

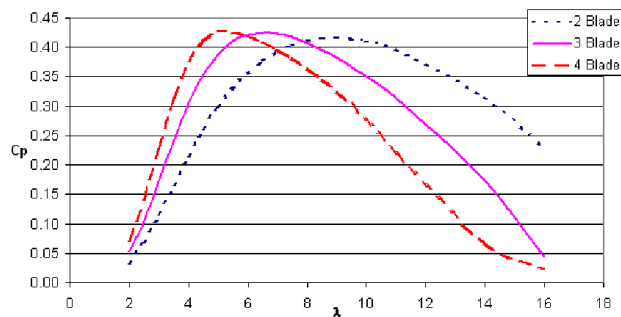


Figure 8. Influence of rotor blades.

5.2. Shape of the rotor blades

The power captured by the rotor will be influenced by the shape of the rotor blades. A mathematically optimum shape can be derived by several ways [3,5]. The common point is that with the rotor momentum theory, C_p of equation (6) is maximised if the axial coefficient has a value of $1/3$ for each section. These mathematical models produce tapered blades with a maximum section next to the hub for low values of λ and extremely slender blades for high values of λ . These mathematical blades can present problems of strength. From the point of view of manufacturing, the aim should be straight-bladed planforms. So, the mathematical shape can be used for a starting point to a more constructible approach with straight lines in some parts of the blade planform, as the one of figure 9.

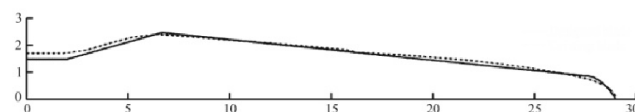
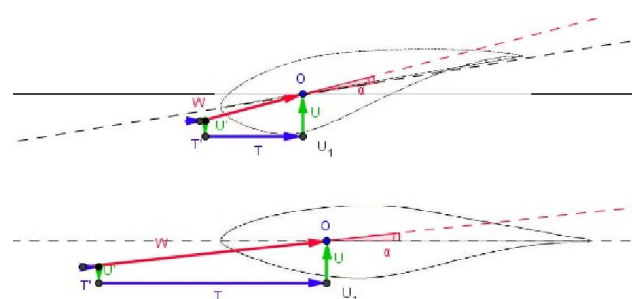


Figure 9. Mathematical and constructible blade shape.

If pitch controlled blades are used, the chord distribution next to the hub is constant since a cylindrical form is used in this part of the blade (figure 1). In the case of fixed blades (figure 2), chord can be increased in this area improving a little C_p and increasing blade strength at this area. Twist angle distribution is also very important to obtain a good behaviour of the airfoils. Since the tangential speed varies along the span and the axial speed is supposed to be constant, the angle of attack will vary importantly from root to tip unless a twist angle distribution is adopted.

Figure 10 shows the twist of the profiles and the velocity polygons at three stations of a blade: $0.3 \cdot R$ at the hub, $0.7 \cdot R$ at the upper part and at 0.9 next to the blade tip. The axial speed is the same in the three cases, but the tangent one varies. The twist is selected so the angle of attack of the three profiles is the same.



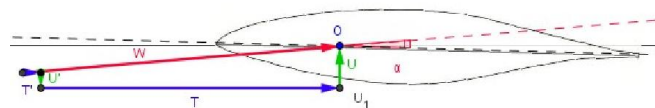


Figure 10. Twist distribution at st. 0.3, 0.7 and 0.9.

The twist is selected according the airfoils characteristics, so the angle of attack can be optimum that means that the profile can produce maximum lift with a minimum drag force.

The twist presents negative values next to the blade tip, and the distribution from blade to tip is a soft curve.

By controlling the twist distribution, the C_p maximum can be sifted to higher or lower tip speed ratios (figure 11). Since the variation of the flow of a tidal turbine is cyclical, the twist can be studied for different operating speeds trying to prevent the stall of a significant part of the blades, in case of fixed pitch blades.

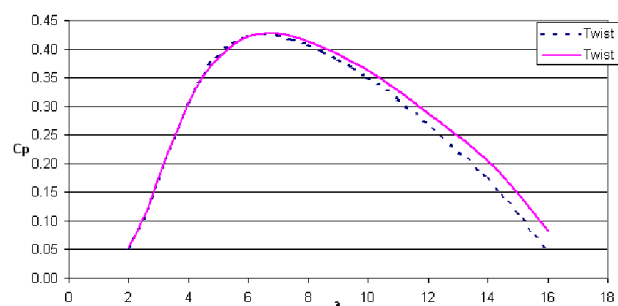


Figure 11. Effect of twist distribution.

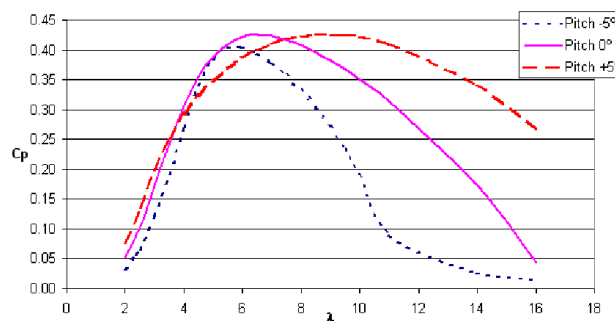


Figure 12. Effect of pitch.

If the blades are pitch controlled, the effect on the C_p can be seen in figure 12. This mechanism can be difficult to maintain under the water and hard to implement on the global design, apart from the necessary control mechanism, but the advantages of such control that allows to maintain the maximum C_p value for different tip speed ratios, are clear on this figure.

The pitch mechanism is used in wind turbines to increase the torque at the starting, and to prevent overpower at high wind speeds. In the case of a well design tidal turbines, overpower is avoided if the maximum tidal speed at the turbine site has been considered in the design.

5.3. Blade sections

The airfoil design is the key for a good behaviour of the rotor since according equations (12) and (13), the total thrust and torque of the rotor depends upon the lift and drag coefficients of the airfoils in which the blades are divided. From the mentioned equations, it can be seen that optimum

torque and thrust will be obtained by maximizing the lift and minimizing the drag forces.

These forces will be a function of the angle of attack (α) and of the Reynolds number of the flow moving into the airfoil. The variation of these coefficients with α for a typical turbine airfoil can be seen in figure 13.

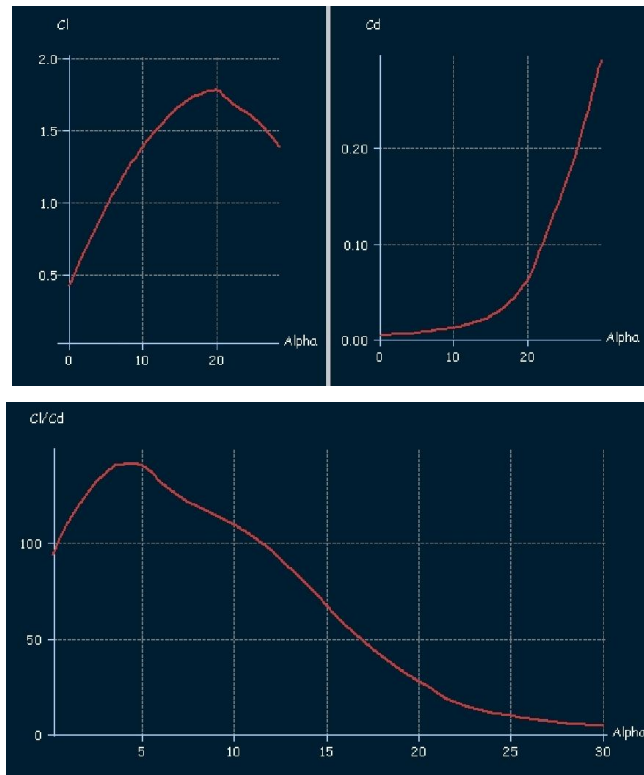


Figure 13. Lift and drag coefficients.

Lift forces rises until a maximum value where stall begins. This means that the airfoil will start to produce turbulence for high values of alpha, the water flow will separate from the surface of the rotor and this will produce a reduction of the lift forces. On the contrary, drag force increases rapidly over a certain angle. So, for any airfoil there will be an optimum point that produces a maximum Cl/Cd and this angle of attack is the target when designing the rotor (in the case of figure 13, this value is about 4°). This is a complex matter since alpha varies along the span of the blade because of rotational effects and changes with the flow condition. This can be seen on the velocity polygon of figure 5.

The lift and drag coefficients will be a function of the Reynolds number that varies along the blade from root to tip. For a water turbine, the Re is over one million. When increasing Re , the lift increases and the drag diminishes, which is positive for water turbines that works in Re number about ten times higher than wind turbines.

The optimum twist of the blade for a given design condition with constant speed U_0 and constant turning speed is obtained when the angle of attack for each airfoil along the blade is next to the optimum angle of attack that produces the maximum Cl / Cd .

In practice this is difficult to find because of the cyclic tide characteristics that produce variations in the entrance flow along the blade both in magnitude (speed profile) and direction (yaw angles). But the mentioned design criteria is the most followed when designing a rotor blade.

When talking about a marine propeller, one has in mind the NACA series (figure 14). The NACA airfoils were developed prior to World War II. All these airfoils were developed for high

Reynolds numbers representative of airplane wings, and suffer from significant laminar separation bubbles when used on wind turbines at much lower Reynolds numbers. These bubbles can lead to large variations in airfoil performance as a function of roughness. These airfoils also lack adequate thickness for the blade-root region to accommodate high root-bending moments.



Figure 14. NACA 4415 and 23015.

Another characteristic needed for turbine airfoils is a reduced sensitivity of the maximum lift coefficient to roughness effects that is of great importance in the marine environment where fouling will be unavoidable.

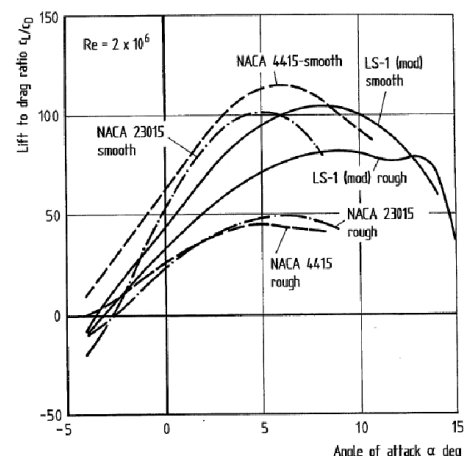


Figure 15. Effect of airfoil roughness.

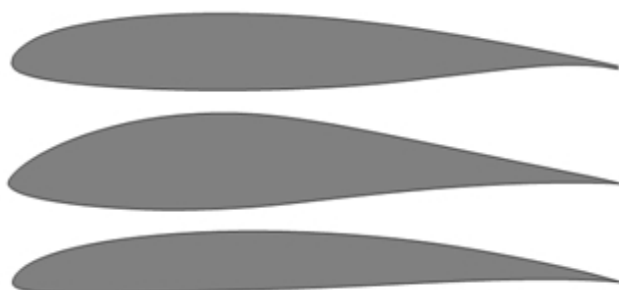


Figure 16. Turbine airfoils.

The increment of surface roughness will produce an increment of the drag, and a diminution of the circulation around the airfoil that will produce a reduction on the lift coefficient. Of course, this is improved with the maintenance of the turbine that in case of water turbine can be difficult and expensive when compared with wind turbines. Figure 15 from [6] shows the effect of roughness on the reduction of the lift coefficient of two NACA profiles and on one specific turbine profile, the LS series, the upper profile of figure 16. This study is made experimentally on wind tunnels by adding sand paper strips to the tested models in a similar way that turbulence stimulators are used in ship models tested in a towing tank.

Normally, turbine profiles have the shape of the ones of figure 16, with the maximum thickness of the upper part moved towards the trailing edge. This way, these profiles exhibit turbulent flow along the entire upper surface just prior to maximum lift, which make these profiles less sensitive to roughness.

By controlling the shape of the lower part, the peak of the lift curve and the stall characteristics can be controlled. The thickness is varied along the blade to accomplish structural design, with the thickest profiles next the hub. Water turbines profiles are thicker than their equivalent wind turbine profiles, because water loads are much higher than wind ones. This produces lower lift and higher drag coefficients than in wind turbines, with the consequent reduction on the power coefficient

curve of a tidal turbine.

5.4. Cavitation

An important difference between wind turbines and marine turbines is that the later has the potential to suffer cavitation, depending on local inflow speed, dynamic forces and depth of immersion as normally studied in ship propellers. With the use of the explained BEM, cavitation can be detected and actions can be made in order to avoid or reduce it.

Cavitation inception is assumed to occur on a rotor section, when its local pressure falls to or bellows the vapour pressure P_v of the water and can be predicted with the pressure distribution around the airfoil section. A cavitation number and a pressure coefficient are usually defined as:

$$\sigma = \frac{P_0 + \rho \cdot g \cdot h - P_v}{\frac{1}{2} \cdot \rho \cdot W^2}; C_p = \frac{P_L - (P_0 + \rho \cdot g \cdot h)}{\frac{1}{2} \cdot \rho \cdot W^2} \quad (15)$$

Where h is the depth of the considered section, and P_L is the dynamic pressure at the section. Cavitation inception can be predicted with the C_p of the upper face of the profile equals σ as depicted in figure 17 where the typical form of C_p is represented as a function of the non-dimensional chord-length of a section.

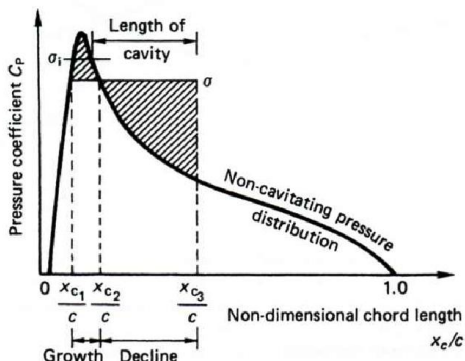


Figure 17. Cavitation inception and extension.

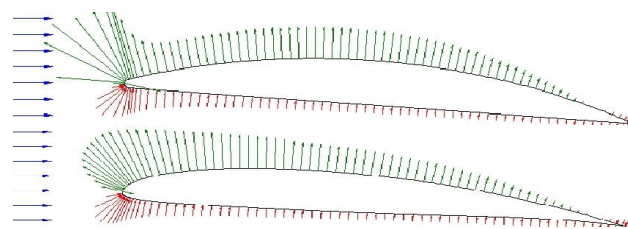


Figure 18. Pressure distributions.

Cavitation will start when $C_p = \sigma$ but will extend for a certain part of the section depending on the pressure distribution that is a function of the airfoil.

Ship propellers normally use segmental sections with a flat pressure side, as the upper profile of figure 18. The lower profile is a typical section of a turbine, with the advantages described in the previous section. Both sections have the same flow characteristics, and one can see how the pressure distribution is more uniform in the case of the ship's propeller type.

When comparing the pressure coefficients of both sections in figure 19, cavitation will start earlier in the segmental section (left) but the extension will be much lower when compared with the second profile (right).

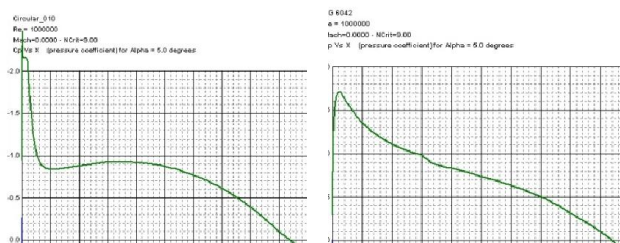
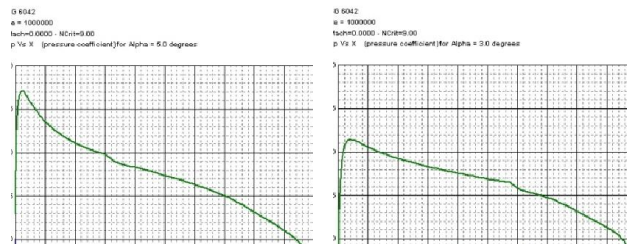


Figure 19. Pressure coefficients.

So, cavitation can be detected with the use of the pressure plots, and the use of different profiles can be considered. Anyway, cavitation can be avoided by altering the twist distribution of the rotor blade: a reduction in the twist will produce a reduction in the angle of attack that has the effect of reducing the pressure, and of course the lift. Figure 20 shows the effect of a 2° reduction in the angle of attack of the lower profile of figure 18.

**Figure 20.** Effect of twist in cavitation.

This modification can eliminate the cavitation of a given section, at the expense of a performance reduction, but cavitation can produce important fatigue and vibration effects on the turbine's structure. The numerical cavitation predictions explained can be used with reasonable confidence for predicting cavitation at the design stage.

6. Conclusions

This paper has presented a simulation method for the hydrodynamic aspects of marine current turbines, through the modelling of the rotor effect with a BEM approach.

Different corrections have been explained to consider the tip and root vortexes and the turbulent wake state where the Glauert empirical correction is used.

The key of a good design is the use of suitable airfoil sections that produce maximum lift with a minimum drag. Comparison with the usual ship's propeller profiles has been made.

The prediction of cavitation has been explained that is important for relatively shallow tip immersion. Cavitation can be avoided with the use of suitable designs and choice of the airfoil sections, and with the global twist distribution of the blades.

Appendices

Table A Below are nomenclatures.

KE	Kinetic energy of the water
BEM	Blade Element Momentum
MCT	Marine Current Turbine
C _p	Power Coefficient
\dot{W}	Power
ρ	Sea Water Density
A	Projected Area
U ₀	Inflow speed
a	Axial induction factor
T	Thrust
Q	Torque
C _t	Thrust coefficient
C _q	Torque coefficient
c	Chord
σ	Solidity

W	Total speed
a'	Circumferential induction factor
Ω	r.p.m.
L	Lift
D	Drag
C_l	Lift coefficient
C_d	Drag coefficient
N	Number of blades
α	Angle of attack
β	Twist angle
Re	Reynolds number

References

- [1] Fox R W and McDonald 2000 *Introduction to Fluid Mechanics* (John Wiley & Sons, London, UK) 5th ed.
- [2] Abbot I H 1959 *Theory of Wing Sections* (Dover Books on Aeronautical Engineering, London, UK) ed. Dover.
- [3] Burton T 2001 *Wind Energy Handbook* (John Wiley & Sons, London, UK)
- [4] Lanzafame R and Messina M 2007 Fluid dynamics wind turbine design: Critical analysis, optimization and application of BEM theory *Renew. Energy* **32** 2291-305
- [5] Liu X, Chen Y and Ye Z Q 2007 Optimization model for rotor blades of horizontal axis wind turbines *Front. Mech. Engin. China* **2** 483-8
- [6] Hau E 2006 *Wind Turbines: Fundamentals, Technologies: Application and Economics* (Springer, London, UK)